AIP | Advances

Fabrication of organic-inorganic perovskite thin films for planar solar cells via pulsed laser deposition

Yangang Liang, Yangyi Yao, Xiaohang Zhang, Wei-Lun Hsu, Yunhui Gong, Jongmoon Shin, Eric D. Wachsman, Mario Dagenais, and Ichiro Takeuchi

Citation: AIP Advances **6**, 015001 (2016); doi: 10.1063/1.4939621
View online: http://dx.doi.org/10.1063/1.4939621
View Table of Contents: http://scitation.aip.org/content/aip/journal/adva/6/1?ver=pdfcov
Published by the AIP Publishing

Fabrication of organic-inorganic perovskite thin films for planar solar cells via pulsed laser deposition

Yangang Liang,[1] Yangyi Yao,[2] Xiaohang Zhang,[1] Wei-Lun Hsu,[2] Yunhui Gong,[1] Jongmoon Shin,[1] Eric D. Wachsman,[1] Mario Dagenais,[2] and Ichiro Takeuchi[1,a]

[1]*Department of Materials Science and Engineering, University of Maryland, College Park, Maryland 20740, USA*

[2]*Department of Electrical and Computer Engineering, University of Maryland, College Park, Maryland 20740, USA*

(Received 1 December 2015; accepted 22 December 2015; published online 4 January 2016)

We report on fabrication of organic-inorganic perovskite thin films using a hybrid method consisting of pulsed laser deposition (PLD) of lead iodide and spin-coating of methylammonium iodide. Smooth and highly crystalline $CH_3NH_3PbI_3$ thin films have been fabricated on silicon and glass coated substrates with fluorine doped tin oxide using this PLD-based hybrid method. Planar perovskite solar cells with an inverted structure have been successfully fabricated using the perovskite films. Because of its versatility, the PLD-based hybrid fabrication method not only provides an easy and precise control of the thickness of the perovskite thin films, but also offers a straightforward platform for studying the potential feasibility in using other metal halides and organic salts for formation of the organic-inorganic perovskite structure. [http://dx.doi.org/10.1063/1.4939621]

I. INTRODUCTION

Organic-inorganic perovskite solar cells (PSCs) have recently emerged as one of the most promising alternatives to silicon based solar cells due to their high efficiency, relatively low cost, and flexibility in materials growth and architecture.[1–8] Many breakthroughs have been made since PSCs were first unveiled in 2009,[1] and a power conversion efficiency (PCE) as high as 20.3% has been reported.[8]

The superior performance of PSCs is based on the unique characteristics of the organic-inorganic perovskite, namely, its relatively high absorption coefficient,[2] tunable bandgap,[9–11] low binding energy of photo-generated electron-hole pairs,[12] high charge-carrier mobilities, and long charge carrier diffusion lengths.[13,14] These factors are of great benefit to the simple planar heterojunction architecture and can lead to low-cost manufacturing with robust device performance.[15]

The high efficiency of PSCs is generally associated with specific synthesis procedures, where controlling the morphology and the grain size of perovskite materials in the device is of utmost importance.[7,8,16,17] Various fabrication methods of the perovskite thin films have been reported to date.[18–21] The synthesis methods can be categorized into the one-step method (e.g. one-step precursor deposition[18] and dual-source vapor deposition[6]) and the two-step method (e.g. the sequential deposition method[19] and vapor-assisted solution process[20]). Compared to the one-step method, the two-step deposition is known to provide better control of the composition, the thickness, and the morphology of the organic-inorganic perovskite films, thus resulting in higher performance PSCs.[8,22,23] In particular, low-temperature all solution-based processes have attracted considerable attention due to their ease of synthesis and low-cost. However, the low solubility of metal halide precursors in organic solvents has been identified as a limiting factor for possible further improvement.[24–26] Thermal evaporation

[a]Electronic mail: takeuchi@umd.edu

methods have been reported as successful in overcoming this issue and synthesizing high quality perovskite thin films.[6,27] Atomic layer deposition (ALD) has also been introduced for growth of halide compounds which are subsequently converted to perovskite thin films by dipping them into a methylammonium iodide (MAI) solution.[28] The typical substrate temperatures of the thermal evaporation method[6] and the ALD method[28] are 325 °C and 150 °C, respectively. Based on these methods, the organic-inorganic perovskite thin films with high purity and crystallinity have been synthesized, they have been used in high-performance devices.[29]

Here, we used pulsed laser deposition (PLD) to fabricate organic-inorganic perovskite thin films, where the substrate temperature is held at room temperature. PLD is a versatile method for fabricating high-quality films of a variety of materials. The main advantages of PLD include its operational simplicity and its non-equilibrium nature which allows stoichiometric mass transfer of materials from the target to the substrate.[30] In PLD, only a few parameters such as the laser energy density, the pulse repetition rate, the substrate temperature, and the deposition pressure need to be adjusted.[30] It is straightforward to apply PLD to the fabrication of multi-layered or composition-spread films by sequential ablation of multiple targets.[31] There have been only a few reports of the use of PLD for deposition of metal halides.[32] Very recently, Bansode et al.[33] prepared perovskite films and solar cells by an off-axis PLD method. In this work, we take advantage of the flexibility of PLD to explore a hybrid method for the fabrication of organic-inorganic perovskites thin films. We show that a PLD-based approach can provide good control of the morphology and the thickness of the perovskite films at room temperature.

II. EXPERIMENTAL SETUP

The fabrication procedure of organic-inorganic perovskite thin films based on our PLD-based hybrid two-step process is schematically shown in Fig. 1. It starts with PLD of PbI_2 at room temperature (Step 1) followed by spin coating of MAI with a subsequent annealing (Step 2). Both Si and glass substrates coated with fluorine doped tin oxide (FTO) are used.

To prepare a PLD target, PbI_2 powders were ground in isopropanol (IPA), baked at 100 °C, pressed as a pellet, and then sintered at 120°C under a nitrogen atmosphere for 8 hours. Fig. 1(a) shows the finished yellow PbI_2 target used in our work. We optimized the laser energy, the repetition rate, and the distance between the substrate and the target to fabricate a smooth PbI_2 film with a relatively low deposition rate. During the PLD of the PbI_2 target, the distance between the substrate and the target was kept at 5.0 cm and a pulsed excimer laser (KrF; λ = 248 nm) was used with an energy density of 0.25 J/cm^2 and a repetition rate of 2 Hz. PbI_2 films were deposited on the substrates in vacuum ($\sim 3.0 \times 10^{-6}$ Torr) at room temperature with the deposition rate of ~0.33 nm/pulse. Step 2 (Fig. 1(c) and 1(d)) consisted of spin-coating of MAI and a subsequent thermal annealing process. Here, we use a conventional spin coating method for the MAI deposition following a procedure described in literature.[5] After optimizing the concentration (MAI in isopropanol), the spin speed, and the drying temperature, a 150 µl MAI solution (40 mg/ml) was spin-coated onto a dried PbI_2 film at 1000 rpm, and the film was then dried at 120 °C for 1 hour to form the $CH_3NH_3PbI_3$ as shown in Fig. 1(e).

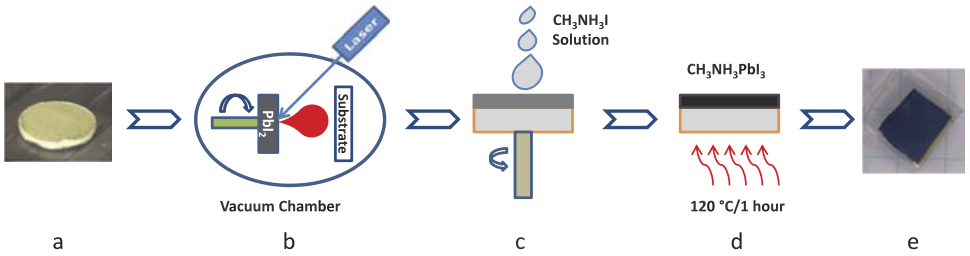

FIG. 1. The schematic representation of the organic-inorganic perovskite thin film formation via pulsed laser deposition. (a) The PbI_2 target used in this work; (b) PbI_2 thin film is deposited on Si or FTO coated glass substrates by the PLD method in a vacuum chamber; (c) The 2-propanol-based CH_3 NH_3I solution is spin-coated onto the PbI_2 thin film; (d) The film is heated at 120 ° for 1 hour to form $CH_3NH_3PbI_3$; (e) The dark $CH_3NH_3PbI_3$ film after annealing.

III. RESULTS AND DISCUSSION

Fig. 2(a) shows the X-ray diffraction (XRD) patterns of a PbI_2 film (after PLD) and a $MAPbI_3$ film (after Step 2) on Si substrates. Polycrystalline and highly oriented nature of the PbI_2 films is evident in Fig. 2(a) (top), where (00l) peaks of PbI_2 are seen,[34] confirming that the (00l) orientated hexagonal lattice of the PbI_2 crystal [space group: P-3m1(164)] has been generated by the PLD method.

For the perovskite phase formed after Step 2, the main XRD peaks of the film indicate that the tetragonal $CH_3NH_3PbI_3$ film is predominantly (110) oriented (Fig. 2(a) (bottom)).[6,7,35] A small XRD peak indicated by an asterisk corresponds to the (001) peak of PbI_2,[34] which is possibly due to the decomposition of $CH_3NH_3PbI_3$ in air or due to residual unreacted PbI_2.[10]

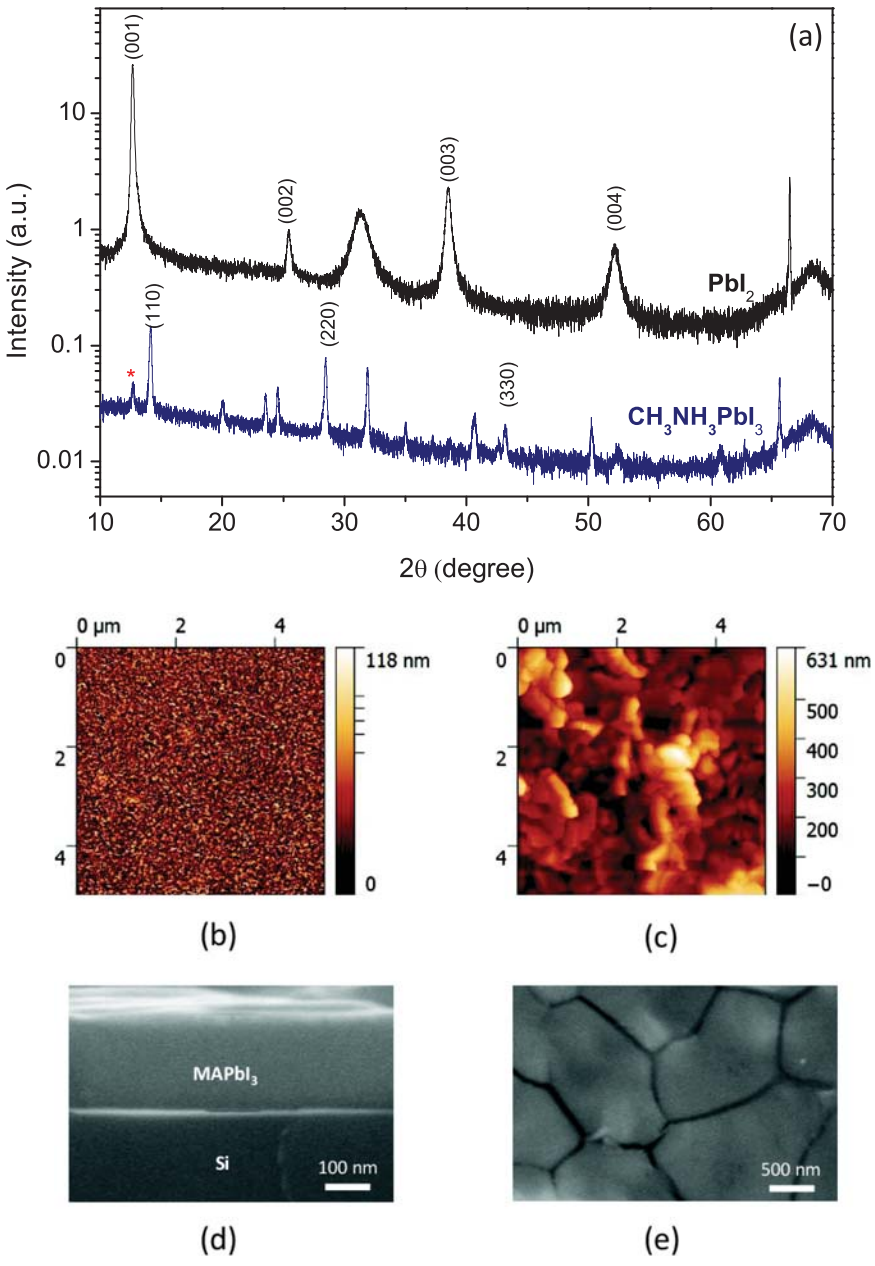

FIG. 2. X-ray diffraction patterns, AFM and SEM images of PbI_2 and $CH_3NH_3PbI_3$ layers. (a) XRD patterns of PbI_2/Si (top), $CH_3NH_3PbI_3$/Si (bottom); (b) AFM image of PLD PbI_2 film on Si; (c) AFM image of $CH_3NH_3PbI_3$ on Si; (d) and (e) Cross-sectional and top view SEM images of $MAPbI_3$ fabricated on Si via PLD method.

We performed atomic force microscopy (AFM) to examine the morphology of our films. A 5 μm × 5 μm AFM image of a PbI_2 film prior to spin-coating of a MAI layer is shown in Fig. 2(b). The root mean square (RMS) roughness is 7.74 nm, indicating that relatively smooth PbI_2 thin films can be prepared by PLD at room temperature. The surface morphology of a completed $CH_3NH_3PbI_3$ film (≈220 nm) was found to show significantly larger RMS roughness of 89 nm (Fig. 2(c)). This enhanced roughness is due to the volume expansion when the perovskite phase is formed during the intercalation of MAI into the PbI_2 layer.[35] This in-situ growth process of organic-inorganic perovskite crystal also leads to a substantial increase in the grain size as shown in Fig. 2(c).

We further characterized the morphology of our perovskite films by scanning electron microscopy (SEM) (Fig. 2(d), 2(e)). The cross-sectional SEM image of $CH_3NH_3PbI_3$ on Si in Fig. 2(d) shows a smooth and a uniform film (220 nm) indicating highly crystalline nature of the organic-inorganic perovskite film. The top-view SEM image shown in Fig. 2(e) indicates complete coverage by the film on the Si substrate surface. The typical grain size ranges from ≈800 nm to ≈1,500 nm. Obtaining large grains is very important for the fabrication of high performance devices because large grains can reduce bulk defects and increase the mobility of charge carriers.[36]

The perovskite films were also fabricated on FTO coated glasses using the same method. Following a procedure described in literatrue,[37] a 50 nm poly(3,4-ethylenedioxythiophene):poly (styrenesulphonate) (PEDOT:PSS) layer was first spin-coated onto FTO coated glasses as the hole transport layer in the device. Following the hybrid PLD process illustrated in Fig. 1, the perovskite phase was formed on the FTO-glass/PEDOT:PSS.

The XRD pattern of a $MAPbI_3$ film (300 nm) fabricated by the PLD-based hybrid method on a FTO coated glass substrate is shown in Fig. 3(a) (top). To perform side-by-side comparison of films made by our hybrid method vs. the conventional method, a $CH_3NH_3PbI_3$ thin film (295 nm) has also been prepared via the standard spin coating of PbI_2 from a dimethylformamide (DMF) solution.[37] The XRD pattern of the latter film is shown in Fig. 3(a) (bottom). The comparison shows that the film made by the PLD-based hybrid method is preferentially (110) oriented, whereas the film made by the conventional spin-coating method shows a relatively weak intensity of (110) peaks. Haruyama et al.[38] reported flat terminations on the (110) and the (001) surfaces are important for the PSC performance.

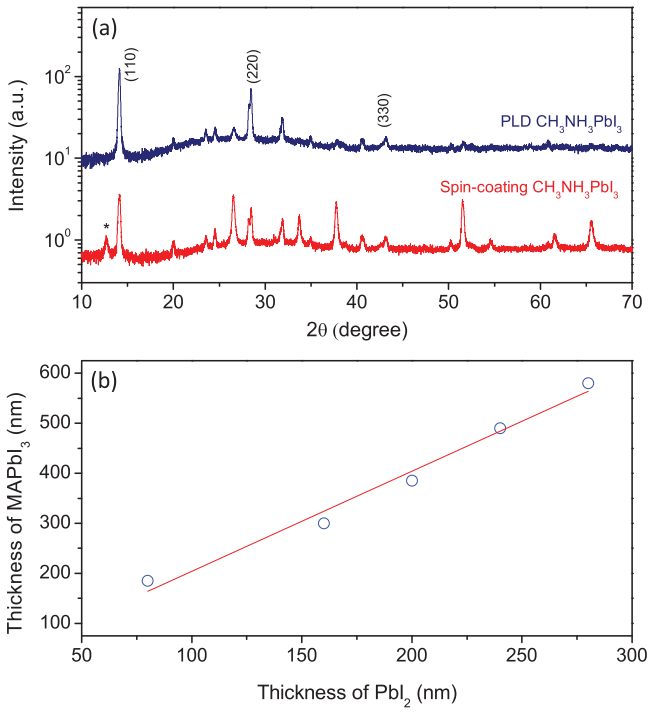

FIG. 3. X-ray diffraction patterns of (a) $CH_3NH_3PbI_3$ films made by the PLD hybrid method (top) and by standard spin-coating-only method (bottom); (b) Perovskite film thickness as a function of the thickness of the PLD PbI_2 film.

Here, the strongly (110) preferred orientation of $CH_3NH_3PbI_3$ made by the hybrid method is attributed to the high quality of the PbI_2 thin film deposited by PLD.

In perovskite thin-film solar cells, a $CH_3NH_3PbI_3$ thin film is used as an absorbing layer. Therefore, the thickness of the $CH_3NH_3PbI_3$ layer is an important device design parameter.[35] To demonstrate precise control of the thickness of the $CH_3NH_3PbI_3$ thin film using the PLD-based hybrid method, we deposited PbI_2 films with different thicknesses and compared them to the thicknesses and the composition of the final $CH_3NH_3PbI_3$ films. When the thickness of the starting PbI_2 thin films is in the range of 80 - 280 nm, the thickness of the final $CH_3NH_3PbI_3$ thin films is found to be in the range of 185 - 580 nm, as determined by profilometry. Interestingly, in all the films synthesized here, the average ratio between the thickness of the $MAPbI_3$ film and the thickness of the starting PbI_2

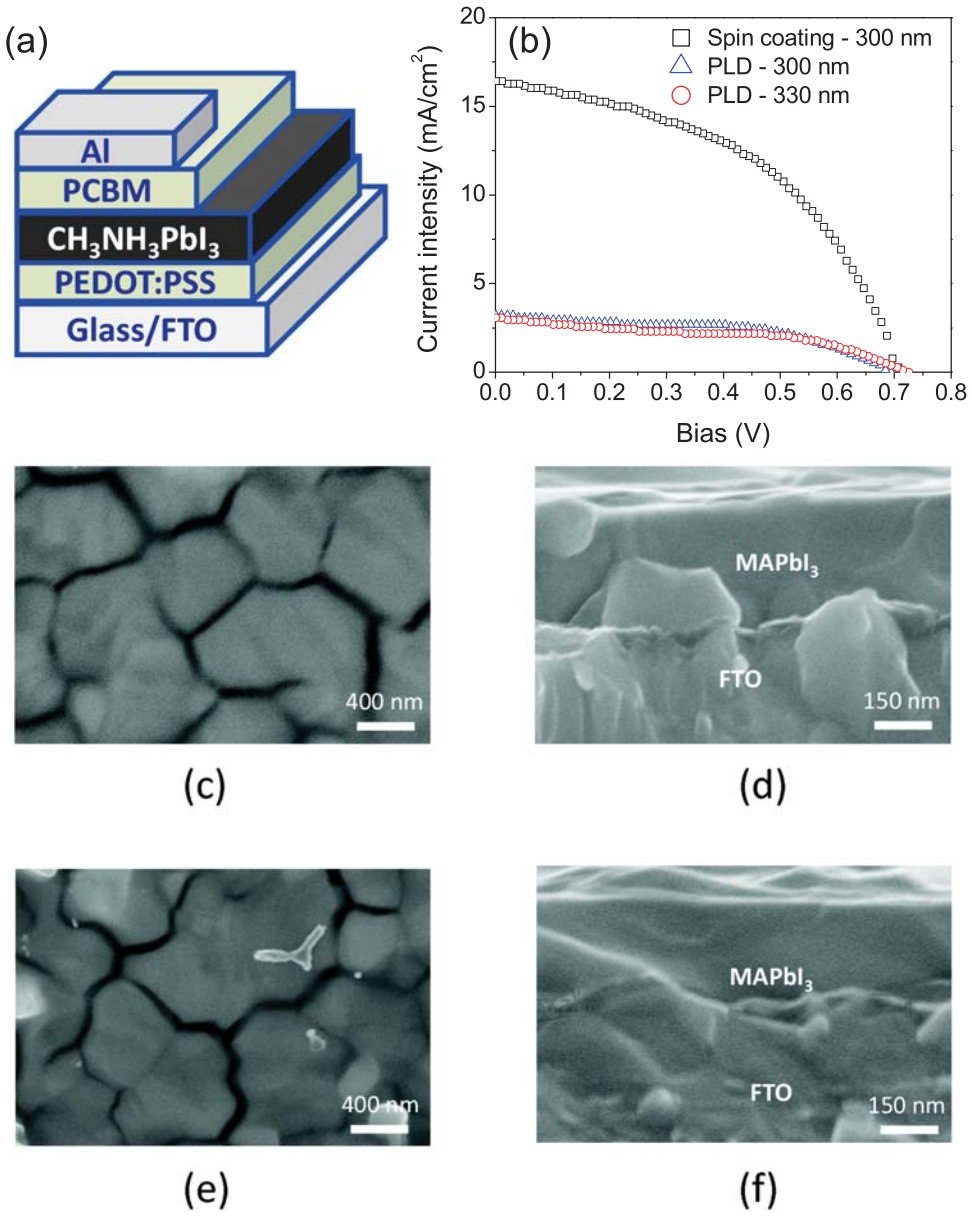

FIG. 4. Planar devices and their performance (a) Device schematic configuration used for this study; (b) J-V curves obtained from the perovskite solar cells fabricated by PLD method ($MAPbI_3$ layer thicknesses: 300 nm and 330 nm) and conventional spin-coating-only method (300 nm $MAPbI_3$ layer); (c) and (d) Top view and cross sectional SEM images of $MAPbI_3$ in a complete solar cell device fabricated via the PLD-based method; (e) and (f) Top view and cross sectional view SEM images of $MAPbI_3$ in a complete solar cell device fabricated via conventional spin-coating-only method.

layer was consistently found to be around 2 (Fig. 3(b)). This agrees well with a recent report[35] and suggests that the excess amount of MAI evaporates during the annealing process. Thus, the PLD of PbI_2 precursor allows the fabrication of organic-inorganic perovskite films with a precisely tailored thickness. In addition, we found that we always see a minor XRD peak at 12.6°((001) peak of PbI_2) when the thickness of PbI_2 is around 240 nm (and the final $MAPbI_3$ is 490 nm).[40] The intensity of this peak increases with increasing thickness of PbI_2 in Step 1. This is due to the fact that there is not enough MAI solution to convert all the PbI_2 into the perovskite under our current recipe (Step 2). We expect that a further optimized MAI spin-coating step may help achieve a complete conversion.

We have fabricated complete cell structures using $MAPbI_3$ films made with our PLD-based hybrid method and also, for comparison, using $MAPbI_3$ films deposited by the conventional spin coating method. In such structures, after the synthesis of a $MAPbI_3$ thin film on PEDOT:PSS coated FTO glasses, an electron transport layer of phenyl-C-butyric acid methyl ester (PCBM) was spin-coated on the surface of $MAPbI_3$, and then a contact electrode of Al was thermally evaporated on the surface of PCBM[37] completing an inverted planar FTO/PEDOT:PSS/$MAPbI_3$/PCBM/Al device structure. A schematic architecture of the device is illustrated in Fig. 4(a). The photovoltaic performance was measured at illumination (AM 1.5G, 100 mA/cm^2). The J-V curves are shown in Fig. 4(b). PCEs of 1.12% and 1.03% were obtained for two cells made by the PLD method with a $MAPbI_3$ layer of 300 nm and 330 nm, respectively. On the other hand, a relatively high PCE (5.45%) was achieved in a cell fabricated through the conventional spin coating method with a 300 nm $MAPbI_3$.

We show the cross-sectional views and the top-view SEM images of $MAPbI_3$ thin films in the two types of cells (one with PLD-based $MAPbI_3$, and another with standard spin-coating $MAPbI_3$). Both films in top-view images (Fig. 4(c), 4(e)) display closely-packed grains with full coverage on the surface of PEDOT:PSS, and there is little difference in the crystallite shape and size between the two. The cross-sectional SEM images (Fig. 4(d), 4(f)) also show that both films are similar in texture and relatively smooth. Based on the XRD and SEM results, we therefore conclude that $MAPbI_3$ thin films fabricated by the PLD method are similar in phase purity and crystallinity compared to those fabricated by the standard spin-coating method, despite the difference in the PCE of the devices. From the J-V curves (Fig. 4(b)), we found that cells made with PLD have similar V_{oc} and the fill factor as the spin-coating cells. This is suggestive of the fact that the films are uniform and pin-hole free,[36–39] and this is consistent with the SEM images. The low PCE is likely due to a dramatically low J_{sc}: a possible reason is that the PEDOT:PSS layer may have deteriorated in the vacuum chamber during the PLD process, reducing the conductivity and resulting in a low J_{sc} and a low V_{oc}. We believe that by further optimizing device parameters and developing materials, achieving higher efficiency values is possible for the PLD-based hybrid deposition process.

IV. CONCLUSION

In summary, we have demonstrated a novel hybrid fabrication process that combines PLD of PbI_2 with subsequent spin coating of MAI to prepare continuous, crystalline, uniform, and compact lead iodide perovskite films with a large grain size. We have demonstrated the versatility of the PLD-based hybrid process in synthesizing $CH_3NH_3PbI_3$ thin films with well-controlled thicknesses. A device based on the PLD process showed a PCE of 1.12%. The hybrid technique described in this work provides a new route for low-temperature fabrication of organic-inorganic perovskite thin films for PSCs with rapid crystallization and good film-thickness control.

ACKNOWLEDGEMENTS

This work was carried out at the Maryland NanoCenter and at the Center for Nanophysics and Advanced Materials at the University of Maryland. The authors thank L. Stevens, E. M. Tennyson, and C. Gong for their help throughout the course of this study.

[1] A. Kojima, K. Teshima, Y. Shirai, and T. Miyasaka, J. Am. Chem. Soc. **131**, 6050 (2009).
[2] J. H. Im, C. R. Lee, J. W. Lee, S. W. Park, and N. G. Park, Nanoscale **3**, 4088 (2011).

[3] H. S. Kim, C. R. Lee, J. H. Im, K. B. Lee, T. Moehl, A. Marchioro, S. J. Moon, R. Humphry-Baker, J. H. Yum, J. E. Moser, M. Grätzel, and N. G. Park, Sci. Rep. **2**, 591 (2012).
[4] M. M. Lee, J. Teuscher, T. Miyasaka, T. N. Murakami, and H. J. Snaith, Science **338**, 643 (2012).
[5] J. H. Heo, S. H. Im, J. H. Noh, T. N. Mandal, C. S. Lim, J. A. Chang, Y. H. Lee, H. J. Kim, A. Sarkar, M. K. Nazeeruddin, M. Grätzel, and S. I. Seok, Nat. Photonics **7**, 487 (2013).
[6] M. Liu, M. B. Johnston, and H. J. Snaith, Nature **501**, 395 (2013).
[7] H. Zhou, Q. Chen, G. Li, S. Luo, T.-B. Song, H.-S. Duan, Z. Hong, J. You, Y. Liu, and Y. Yang, Science **345**, 542 (2014).
[8] N. J. Jeon, J. H. Noh, W. S. Yang, Y. C. Kim, S. Ryu, J. Seo, and S. I. Seok, Nature **517**, 476 (2015).
[9] J. H. Noh, S. H. Im, J. H. Heo, T. N. Mandal, and S. I. Seok, Nano Letters **13**, 1764 (2013).
[10] N. Pellet, P. Gao, G. Gregori, T-Y. Yang, M. K. Nazeeruddin, J. Maier, and M. Grätzel, Angew. Chem. Int. Ed. **53**, 3151 (2014).
[11] Y. Ogomi, A. Morita, S. Tsukamoto, T. Saitho, N. Fujikawa, Q. Shen, T. Toyoda, K. Yoshino, S. S. Pandey, T. Ma, and S. Hayase, J. Phys. Chem. Lett. **5**, 1004 (2014).
[12] K. Tanaka, T. Takahashi, T. Ban, T. Kondo, K. Uchida, and N. Miura, Solid State Communications **127**, 619 (2003).
[13] S. D. Stranks, G. E. Eperon, G. Grancini, C. Menelaou, M. J. P. Alcocer, T. Leijtens, L. M. Herz, A. Petrozza, and H. J. Snaith, Science **342**, 341 (2013).
[14] G. Xing, N. Mathews, S. Sun, S. S. Lim, Y. M. Lam, M. Grätzel, S. Mhaisalkar, and T. C. Sum, Science **342**, 344 (2013).
[15] W. A. Laban and L. Etgar, Energy Environ. Sci. **6**, 3249 (2013).
[16] J.-H. Im, I.-H. Jang, N. Pellet, M. Grätzel, and N.-G. Park, Nat. Nanotechnology **9**, 927 (2014).
[17] P. Gao, M. Gärtzela, and M. K. Nazeeruddin, Energy Environ. Sci. **7**, 2448 (2014).
[18] G. E. Eperon, V. M. Burlakov, P. Docampo, A. Goriely, and H. J. Snaith, Adv. Funct. Mater. **24**, 151 (2014).
[19] S. Pang, H. Hu, J. Zhang, S. Lv, Y. Yu, F. Wei, T. Qin, H. Xu, Z. Liu, and G. Cui, Chem. Mater. **26**, 1485 (2014).
[20] Q. Chen, H. Zhou, Z. Hong, S. Luo, H. S. Duan, H. H. Wang, Y. Liu, G. Li, and Y. Yang, J. Am. Chem. Soc. **136**, 622 (2013).
[21] A. H. Ip, L. N. Quan, M. M. Adachi, J. J. McDowell, J. Xu, D. H. Kim, and E. H. Sargent, Appl. Phys. Lett. **106**, 143902 (2015).
[22] S. R. Raga, M.-C. Jung, M. V. Lee, M. R. Leyden, Y. Kato, and Y. Qi, Chem. Mater. **27**, 1597 (2015).
[23] A. T. Barrows, A. J. Pearson, C. K. Kwak, A. D. F. Dunbar, A. R. Buckley, and D. G. Lidzey, Energy Environ. Sci. **7**, 2944 (2014).
[24] J. Burschka, N. Pellet, S.-J. Moon, R. Humphry-Baker, P. Gao, M. K. Nazeeruddin, and M. Grätzel, Nature **499**, 316 (2013).
[25] D. Liu and T. L. Kelly, Nat. Photonics **8**, 133 (2014).
[26] B. Conings, L. Baeten, C. De Dobbelaere, J. D'Haen, J. Manca, and H.-G. Boyen, Adv. Mater. **26**, 2041 (2014).
[27] Mo. M. Tavakoli, H. Aashuri, A. Simchi, S. Kalytchuk, and Z. Fan, J. Phys. Chem. C **119**, 18886 (2015).
[28] B. R. Sutherland, S. Hoogland, M. M. Adachi, P. Kanjanaboos, C. T. O. Wong, J. J. McDowell, J. Xu, O. Voznyy, Z. Ning, A. J. Houtepen, and E. H. Sargent, Adv. Mater. **27**, 53 (2015).
[29] T. Salim, S. Sun, Y. Abe, A. Krishna, A. C. Grimsdale, and Y. M. Lam, J. Mater. Chem. A **3**, 8943 (2015).
[30] H. M. Christen and G. Eres, J. Phys.: Condens. Matter **20**, 264005 (2008).
[31] H. Koinuma and I. Takeuchi, Nature Materials **3**, 429 (2004).
[32] B. L. Zhu and X. Z. Zhao, Phys. Status Solidi A **208**, 91 (2011).
[33] U. Bansode, R. Naphade, O. Game, S. Agarkar, and S. Ogale, J. Phys. Chem. C **119**, 9177 (2015).
[34] M. Shkir, H. Abbas, Siddhartha, and Z. R. Khan, Journal of Physics and Chemistry of Solids **73**, 1309 (2012).
[35] D. Liu, M. K. Gangishetty, and T. L. Kelly, J. Mater. Chem. A **2**, 19873 (2014).
[36] W. Nie, H. Tsai, R. Asadpour, J.-C. Blancon, A. J. Neukirch, G. Gupta, J. J. Crochet, M. Chhowalla, S. Tretiak, M. A. Alam, H.-L. Wang, and A. D. Mohite, Science **30**, 522 (2015).
[37] Z. Xiao, C. Bi, Y. Shao, Q. Dong, Q. Wang, Y. Yuan, C. Wang, Y. Gao, and J. Huang, Energy Environ. Sci. **7**, 2619 (2014).
[38] J. Haruyama, K. Sodeyama, L. Han, and Y. Tateyama, J. Phys. Chem. Lett. **5**, 2903 (2014).
[39] K. M. Boopathi, M. Ramesh, P. Perumal, Y.-C. Huang, C.-S. Tsao, Y.-F. Chen, C.-H. Lee, and C.-W. Chu, J. Mater. Chem. A **3**, 9257 (2015).
[40] See supplementary material at http://dx.doi.org/10.1063/1.4939621 for XRD patterns of the $CH_3NH_3PbI_3$ films with varying thickness on FTO coated glasses in FIG S2.